

Article

Synthesis and 2D-QSAR Study of Active Benzofuran-Based Vasodilators

Nagy M. Khalifa ^{1,2} , Aladdin M. Srouf ^{2,*†}, Somaia S. Abd El-Karim ^{2,†}, Dalia O. Saleh ^{3,†} and Mohamed A. Al-Omar ¹ 

¹ Pharmaceutical Chemistry Department, Drug Exploration & Development Chair (DEDC), College of Pharmacy, King Saud University, Riyadh 11451, Saudi Arabia; nagykhalifa@hotmail.com (N.M.K.); Malomar1@KSU.EDU.SA (M.A.A.-O.)

² Therapeutical Chemistry Department, National Research Centre, Dokki, Giza 12622, Egypt; somaia_elkarim@hotmail.com

³ Pharmacology Department, National Research Centre, Dokki, Giza 12622, Egypt; doabdelfattah@yahoo.com

* Correspondence: aladdinsrouf@gmail.com; Tel.: +20-2-01229749596

† These authors contributed equally to this work.

Received: 18 September 2017; Accepted: 22 October 2017; Published: 26 October 2017

Abstract: A new series of 2-alkyloxy-pyridine-3-carbonitrile-benzofuran hybrids (**4a–x**) was synthesized. All the new derivatives were examined via the standard technique for their vasodilation activity. Some of the investigated compounds exhibited a remarkable activity, with compounds **4w**, **4e**, **4r**, **4s**, **4f** and **4g** believed to be the most active hits in this study with IC₅₀ values 0.223, 0.253, 0.254, 0.268, 0.267 and 0.275 mM, respectively, compared with amiodarone hydrochloride, the reference standard used (IC₅₀ = 0.300 mM). CODESSA PRO was employed to obtain a statistically significant 2-Dimensional Quantitative Structure Activity Relationship (2D-QSAR) model describing the bioactivity of the newly synthesized analogs ($N = 24$, $n = 4$, $R^2 = 0.816$, $R^2_{cv,OO} = 0.731$, $R^2_{cv,MO} = 0.772$, $F = 21.103$, $s^2 = 6.191 \times 10^{-8}$).

Keywords: benzofuran; vasodilation activity; 2D-QSAR; amiodarone hydrochloride

1. Introduction

Hypertension is the most common cardiovascular and cerebrovascular disorder representing the major risk factor for endothelial dysfunctions [1,2]. Worldwide, one of every three adults is reported to have high blood pressure, which is responsible for half of the mortalities related to stroke and heart disease [2,3]. Under hypertensive conditions, many functional organs can suffer irreparable lesions [4,5]. Essential hypertension is a common trait caused by many factors and it increases the risk of cardiovascular (heart attacks), cerebrovascular (stroke), peripheral artery, rheumatic heart, congenital heart, heart failure and renal diseases [6–8]. A benzofuran-containing compound, amiodarone, is one of the most therapeutically important antiarrhythmic drugs for various types of cardiac dysrhythmias [9,10] (Figure 1). Though the responsible pharmacological mechanisms of amiodarone's antiarrhythmic effects are not settled [11], it has an extreme effect on various ionic currents [12], as well as sodium, calcium and potassium fluxes. These actions are interrelated in a complex way, but are of prime importance for its activity. Amiodarone also possesses coronary and peripheral vasodilator properties [11]—this appears to be mainly due to a release of nitric oxide (NO). Moreover, it expands the precompressed in vivo human hand veins through the activation of NO synthase and blockade of α -adrenergic mechanisms as a venodilator [13,14], and amiodarone's analog KB130015 (Figure 1) activates the BK_{Ca} channels, which relaxes vascular smooth muscle cells. KB130015 is a novel BK_{Ca} activator—its efficacy is based on the subunit composition of the channel complex [15]. Dronedarone as well as KB130015 (Figure 1) is a noniodinated congener of amiodarone that has been developed and

approved by FDA (Food and Drug Administration) to avoid the limiting iodine-associated adverse effects of the commercially used amiodarone. Additionally, dronedarone displays antiadrenergic properties, atrial flutter and atrial fibrillation [16]. Consequently, the stimulation of coronary dilation by dronedarone involving a dual mechanism, putative Ca^{2+} channels inhibition and stimulation of NO synthase pathway [16,17]. Benzofurans are naturally existing scaffolds [18], associated with a broad range of chemotherapeutic properties [19–25]. Nicotinate esters are very interesting vasodilatory active heterocycles [26,27], also, many nicotinate analogs such as, micinicate, hepronicate and inositol nicotinate are of significant vasodilating activity [28], (Figure 1).

In the present study, we designed and synthesized some novel hybrids of pyridine-3-carbonitriles and benzofuran-pyrazole functions, attributed to the fact that, pyridine-3-carbonitriles are interesting agents in developing new active hits due to the recognition of bioisosterism with the nicotinate analogs where the acid/ester function is just replaced by a cyano group [28]. Furthermore, it is known that the benzofuran-pyrazole hybrid is of considerable vasorelaxant interest [29], this may due to the belief that the aliphatic secondary amine side chain of amiodarone might be responsible for its vasodilation activity [30,31]. Thus, the insertion of a pyrazole ring system in this scaffold may widen new pharmacological active hits with higher potency and fewer side effects. In addition, studying the two-dimensional quantitative structure activity relationships (2D-QSAR) for the newly synthesized analogs explored the controlling factors governing the observed pharmacological properties as well as validated of the observed activity of the new chemical entities.

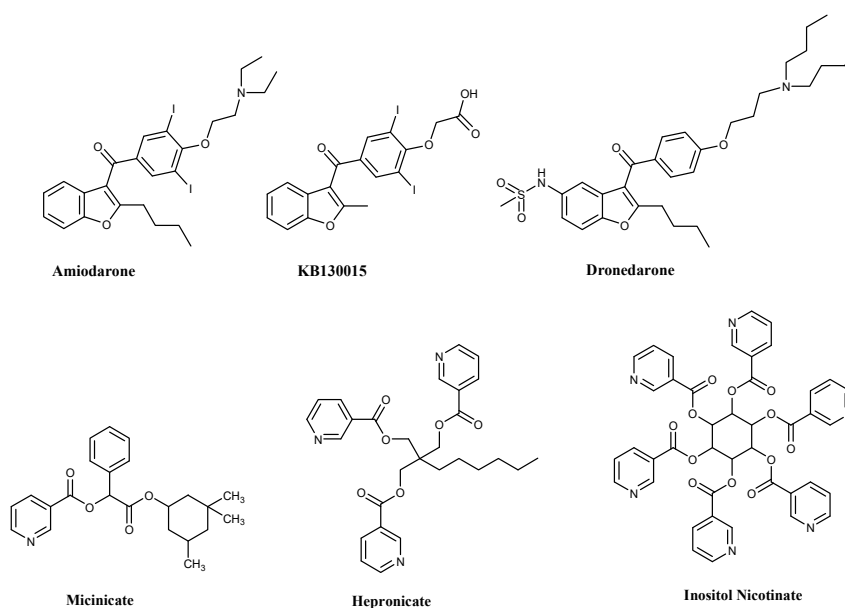


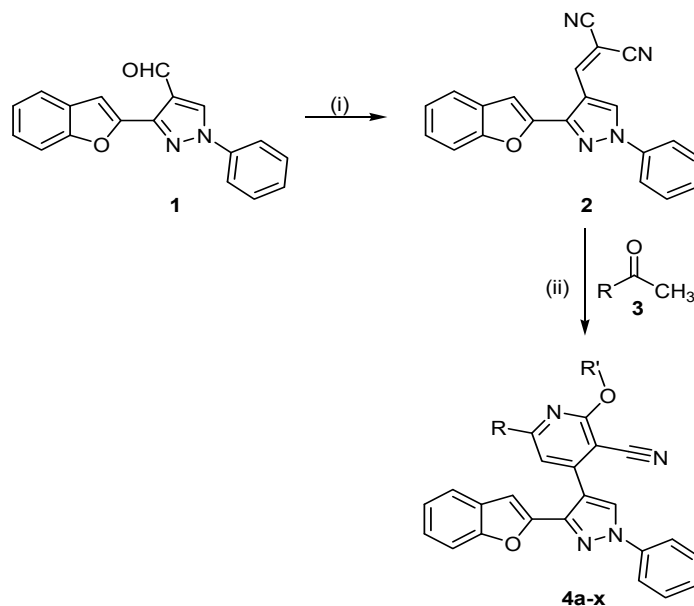
Figure 1. Structures of some active vasodilating agents.

2. Results and Discussion

2.1. Chemistry

The assumed synthetic approach to obtain target derivatives is illustrated in (Scheme 1). Treating 2-acetylbenzofuran, the key starting compound in this study, with phenyl hydrazine afforded the corresponding semihydrazone derivative which undergo formylation via Vilsmeier–Haack reaction to give 3-(benzofuran-2-yl)-1-phenyl-1H-pyrazole-4-carbaldehyde (1) [32]. The formed carbaldehyde 1 was treated with malononitrile in refluxing ethanol to give 2-((3-(benzofuran-2-yl)-1-phenyl-1H-pyrazol-4-yl)-methylene)malononitrile (2). Adopting the reported procedure [32], the required 2-alkoxy-pyridine-3-carbonitrile derivatives 4a–x were synthesized via the condensation reaction of aromatic ketones 3a–l with ylidenemalononitrile 2 and sodium alkoxide of the corresponding alcohol

(Scheme 1). As a representative example, the IR spectrum of compound **4a** shows a strong stretching vibration band at $\nu = 2213 \text{ cm}^{-1}$ for nitrile group. $^1\text{H-NMR}$ spectrum of **4a** exhibits a characteristic signal at $\delta = 4.23 \text{ ppm}$ referring to the methoxide group, while the pyridinyl H-5 appeared as singlet peak at $\delta = 8.42 \text{ ppm}$. $^{13}\text{C-NMR}$ spectrum of **4a** reveals the presence of a methoxide carbon at $\delta = 54.7 \text{ ppm}$, pyridinyl C-3, C-5 and nitrile carbon signals appeared at $\delta = 93.5, 105.8, \text{ and } 114.6 \text{ ppm}$, respectively. Mass spectrum (EI) of **4a** reveals the molecular ion peak 482.27 with relative intensity value 30.7%. The established structures of all new chemical entities **4a–x** were certified by their microanalyses and spectral data (IR, $^1\text{H-NMR}$, $^{13}\text{C-NMR}$ and EI-MS).



3a; R = Ph
3b; R = 4-ClC₆H₄
3c; R = 4-BrC₆H₄
3d; R = 4-FC₆H₄
3e; R = 4-H₃CC₆H₄
3f; R = 4-H₃COC₆H₄
3g; R = 1,2,3,4-Tetrahydronaphthalen-6-yl
3h; R = 2-Pyrrolyl
3i; R = 2-Furanyl
3j; R = 2-Thienyl
3k; R = 2-Pyridinyl
3l; R = 1-Methyl-1H-benzo[d]imidazol-2-yl

4a; R = Ph
4b; R = Ph
4c; R = 4-ClC₆H₄
4d; R = 4-ClC₆H₄
4e; R = 4-BrC₆H₄
4f; R = 4-BrC₆H₄
4g; R = 4-FC₆H₄
4h; R = 4-FC₆H₄
4i; R = 4-H₃CC₆H₄
4j; R = 4-H₃CC₆H₄
4k; R = 4-H₃COC₆H₄
4l; R = 4-H₃COC₆H₄
4m; R = 1,2,3,4-Tetrahydronaphthalen-6-yl, R' = Me
4n; R = 1,2,3,4-Tetrahydronaphthalen-6-yl, R' = Et
4o; R = 2-Pyrrolyl, R' = Me
4p; R = 2-Pyrrolyl, R' = Et
4q; R = 2-Furanyl, R' = Me
4r; R = 2-Furanyl, R' = Et
4s; R = 2-Thienyl, R' = Me
4t; R = 2-Thienyl, R' = Et
4u; R = 2-Pyridinyl, R' = Me
4v; R = 2-Pyridinyl, R' = Et
4w; R = 1-Methyl-1H-benzo[d]imidazol-2-yl, R' = Me
4x; R = 1-Methyl-1H-benzo[d]imidazol-2-yl, R' = Et

Reagents and Conditions: (i) CNCH₂CN/Ethanol/r.t./6 h, 75%; (ii) alcohol/Na/r.t./33.3–45.3%.

Scheme 1. Synthetic route of 2-alkoxy-pyridine-3-carbonitrile derivatives **4a–x**.

2.2. Biological Evaluation

2.2.1. Vasodilation Properties

Vasodilation properties of the synthesized 2-alkyloxy-pyridine-3-carbonitrile derivatives **4a–x** were inspected applying the separated thoracic aortic rings of mice pre-contracted by norepinephrine hydrochloride according to the standard method [33] using amiodarone hydrochloride as a standard reference. The observed data (Table 1), (Figures S1 and S2 of Supplementary Materials) reveal that most the new chemical entities reveal remarkable vasodilation properties. Meanwhile, compounds **4w**, **4e**, **4r**, **4s**, **4f** and **4g** exhibit significant activity (IC_{50} , is the required concentration for 50% lessening of maximal norepinephrine. HCl induced contracture = 0.223, 0.253, 0.254, 0.268, 0.267 and 0.275 mM, respectively), that seems more potent than the used reference standard in the present study (IC_{50} = 0.300 mM). The 2D-QSAR study was initiated to recognize the observed bioactivities and concluding the most important factors that manage the pharmacological properties. Currently, throughout the observed vasodilator activities of the new chemical entities, few Structure activity relationship (SAR) rules could be achieved, the presence of a methoxy group at the 2-position of 3-pyridinecarbonitriles enhances the vasodilation activity more than the ethoxy group, as shown in all of the tested analogs. Compounds **4k** and **4q** (IC_{50} = 0.428, 0.321 mM, respectively) are exceptions. Benzimidazole ring systems attached to pyridine-C₅ seems appropriate for designing vasodilation active hits (IC_{50} = 0.223, 0.299 mM) compared with the corresponding substituted phenyl ring systems or other heterocycles. Thus, the combination of benzimidazole, pyridine and benzofuran has the potential to be developed into potent vasorelaxant active targets.

Table 1. Vasodilatory activity IC_{50} (mM) in rat thoracic aortic rings.

Entry	Compound	R	R'	Potency (IC_{50}), mM
1	4a	Ph	Me	0.281
2	4b	Ph	Et	0.343
3	4c	4-ClC ₆ H ₄	Me	0.295
4	4d	4-ClC ₆ H ₄	Et	0.397
5	4e	4-BrC ₆ H ₄	Me	0.253
6	4f	4-BrC ₆ H ₄	Et	0.267
7	4g	4-FC ₆ H ₄	Me	0.275
8	4h	4-FC ₆ H ₄	Et	0.330
9	4i	4-H ₃ CC ₆ H ₄	Me	0.330
10	4j	4-H ₃ CC ₆ H ₄	Et	0.452
11	4k	4-H ₃ COC ₆ H ₄	Me	0.322
12	4l	4-H ₃ COC ₆ H ₄	Et	0.291
13	4m	1,2,3,4-Tetrahydronaphthalen-6-yl	Me	0.286
14	4n	1,2,3,4-Tetrahydronaphthalen-6-yl	Et	0.337
15	4o	2-Pyrrolyl	Me	0.356
16	4p	2-Pyrrolyl	Et	0.400
17	4q	2-Furanyl	Me	0.321
18	4r	2-Furanyl	Et	0.254
19	4s	2-Thienyl	Me	0.268
20	4t	2-Thienyl	Et	0.298
21	4u	2-Pyridinyl	Me	0.333
22	4v	2-Pyridinyl	Et	0.370
23	4w	1-Methyl-1H-benzo[d]imidazol-2-yl	Me	0.223
24	4x	1-Methyl-1H-benzo[d]imidazol-2-yl	Et	0.299
25	Amiodarone.HCl	-	-	0.300

To validate and understand the observed pharmacological activities and to detect the factors that control the activities, the 2D-QSAR study was initiated via the CODESSA PRO package. Molecular descriptors of the 2D-QSAR correlating the chemical structure(s) and property values expressed as $1/IC_{50}$ μ M are presented in Table 2, arranged on their level of significance (*t*-criterion). The descriptors were acquired using the BMLR (Best Multiple Linear Regression) method. The first descriptor

controlling the BMLR-QSAR model based on its t -criterion value ($t = 7.789$) is maximum e–e repulsion for bond C–O which is a semiempirical descriptor. Electron–electron repulsion between two given atoms is determined by Equation (1) [34].

$$E_{ee}(AB) = \sum_{\mu, \nu \in A} \sum_{\lambda, \sigma \in B} P_{\mu\nu} P_{\lambda\sigma} \langle \mu\nu | \lambda\sigma \rangle \quad (1)$$

where, A stands for a given atomic species, B is another atomic species $P_{\mu\nu}$, $P_{\lambda\sigma}$ is density matrix elements over atomic basis $\{\mu\nu\lambda\sigma\}$, $\langle \mu\nu | \lambda\sigma \rangle$ is the electron repulsion integrals on atomic basis $\{\mu\nu\lambda\sigma\}$. The second important descriptor controlling the BMLR-QSAR model ($t = -3.637$) is surface-weighted charged partial-negative charged surface area ($WNSA1$) weighted PNSA ($PNSA1 \times TMSA/1000$) (MOPAC PC) (charge-related descriptor). Surface-weighted charged partial negative-charged surface area ($WNSA1$) is calculated by Equation (2) [34].

$$WNSA1 = \frac{PNSA1 \cdot TMSA}{1000} \quad (2)$$

where, $PNSA1$ stands for partial negatively charged molecular surface area, $TMSA$ for total molecular surface area. The third descriptor controlling BMLR-QSAR model ($t = -5.670$) is the fractional hydrogen bonding acceptor ability of the molecule $FHACA1$, which is also a charge-related descriptor determined by Equation (3) [34].

$$FHACA1 = \frac{HACA1}{TMSA} \quad (3)$$

where, $HACA1$ is hydrogen bonding acceptor ability, $TMSA$ is the total molecular surface area. The fourth descriptor controlling BMLR-QSAR model ($t = -6.241$) is a semiempirical descriptor, maximum e–n attraction for bond C–N, is determined by Equation (4) [34].

$$E_{ne}(AB) = \sum_B \sum_{\mu, \nu \in A} P_{\mu\nu} \langle \mu | \frac{Z_B}{R_{iB}} | \nu \rangle \quad (4)$$

where, A stands for a given atomic species, B is another atomic species $P_{\mu\nu}$ is density matrix elements over atomic basis $\{\mu\nu\}$, Z_B for charge of atomic nucleus B , R_{iB} for distance between the electron and atomic nucleus B , $\langle \mu | \frac{Z_B}{R_{iB}} | \nu \rangle$ for electron–nuclear attraction integrals on atomic basis $\{\mu\nu\}$. The correlation between the observed and predicted vasodilation activities is represented in Figure 2. The descriptor values for each respective compound are exhibited in Table S1 of Supplementary Material.

Table 2. Descriptors of the BMLR-QSAR model for the vasodilatory active compounds.

Entry	ID	Coefficient	s	t	Descriptor
$N = 24, n = 4, R^2 = 0.816, R^2_{cv,OO} = 0.731, R^2_{cv,MO} = 0.772, F = 21.103, s^2 = 6.191 \times 10^{-8}$					
1	0	1.464	0.244	6.009	Intercept
2	D_1	0.0004	4.751×10^{-5}	7.789	Max. e–e repulsion for bond C–O
3	D_2	-7.1825×10^{-6}	1.975×10^{-6}	-3.637	$WNSA-1$ Weighted PNSA ($PNSA1 \cdot TMSA/1000$) (MOPAC PC)
4	D_3	-0.255	0.045	-5.670	$FHACA$ Fractional HACA ($HACA1/TMSA$) (MOPAC PC)
5	D_4	-0.0043	0.001	-6.241	Max. e–n attraction for bond C–N
$1/IC_{50} (\mu M) = 1.464 + (0.0004 \times D_1) - [(7.1825 \times 10^{-6}) \times D_2] - (0.255 \times D_3) - (0.0043 \times D_4)$					

The reliability and statistical relevance of the attained BMLR-QSAR model is examined by internal validation technique, which is an appropriate technique due to the limited data points of the present study [35–37]. Internal validation is applied by the CODESSA PRO employing both Leave One Out (LOO), which involves developing a number of models with one example omitted at a time, and Leave Many Out (LMO) that develops a number of models with many data points omitted at a time (up to 20% of the total data points). The observed correlations attributed to the internal

validation techniques are $R^2_{cv,OO} = 0.731$, $R^2_{cv,MO} = 0.772$. Both of them are significantly correlated with the R^2 value of the attained QSAR model ($R^2 = 0.816$). Standard deviation of the regressions ($s^2 = 6.191 \times 10^{-8}$) and Fisher test value ($F = 21.103$) are also statistical parameters supporting the QSAR model. The predicted/estimated IC_{50} values of the new chemical entities according to the achieved BMLR-QSAR model are displayed in Table 3. The obtained results revealed that the most potent analogue among all the tested hybrids, compound **4w**, shows error value (difference between estimated and observed IC_{50} values) = -0.4 . Additionally, the high potent analogues synthesized **4a–i**, relative to the standard reference, amiodarone hydrochloride ($IC_{50} = 300 \mu\text{M}$), also exhibited estimated bioproperties matched with their observed potencies ($IC_{50} = 253–397 \mu\text{M}$, $253–392 \mu\text{M}$, corresponding to the observed and predicted values respectively, error = $0–40$). Compound **4j** is the only exception with high error value = 83 with ($IC_{50} = 452, 369 \mu\text{M}$, for observed and predicted bio-data, respectively). This compound is exhibited as an outlier (Figure 2) and shows the lowest vasodilation properties among all the synthesized hybrids. From all the above, it can be concluded that the achieved BMLR-QSAR model is statistically significant and also supported by the matched correlations due to the observed and predicted bio-observations. Success of this study can be attributed to the homogeneity of chemical structural entities. Additionally, the achieved model can be adopted for optimizing hits of high potency relative to the standard reference used based on the hybrid design mentioned in the present study.

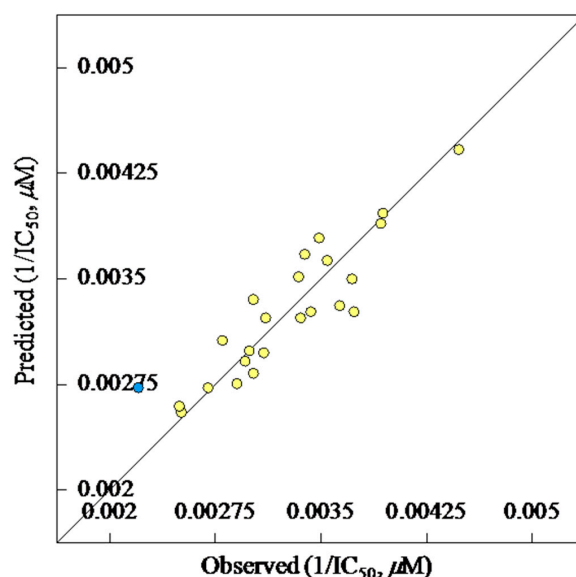


Figure 2. BMLR-QSAR model plot of correlations, the yellow dots are representing the observed vs. predicted vasodilatory active agents for all compounds, while the blue dot is represent an outlier compound (compound **4j**).

Table 3. Observed and estimated/predicated values of the vasodilatory active compounds according to the BMLR-QSAR model.

Entry	Compd.	R	R'	Observed IC_{50} , μM	Estimated IC_{50} , μM	Error
1	4a	Ph	Me	281	276	5
2	4b	Ph	Et	343	363	-20
3	4c	4-ClC ₆ H ₄	Me	295	272	23
4	4d	4-ClC ₆ H ₄	Et	397	392	5
5	4e	4-BrC ₆ H ₄	Me	253	253	0
6	4f	4-BrC ₆ H ₄	Et	267	307	-40
7	4g	4-FC ₆ H ₄	Me	275	303	-28
8	4h	4-FC ₆ H ₄	Et	330	354	-24
9	4i	4-H ₃ CC ₆ H ₄	Me	330	299	31
10	4j	4-H ₃ CC ₆ H ₄	Et	452	369	83

Table 3. Cont.

Entry	Compd.	R	R'	Observed IC ₅₀ , μM	Estimated IC ₅₀ , μM	Error
11	4k	4-H ₃ COC ₆ H ₄	Me	322	337	−15
12	4l	4-H ₃ COC ₆ H ₄	Et	291	307	−16
13	4m	1,2,3,4-Tetrahydronaphthalen-6-yl	Me	286	265	21
14	4n	1,2,3,4-Tetrahydronaphthalen-6-yl	Et	337	344	−7
15	4o	2-Pyrrolyl	Me	268	286	−18
16	4p	2-Pyrrolyl	Et	298	311	−13
17	4q	2-Furanyl	Me	321	310	11
18	4r	2-Furanyl	Et	254	257	−3
19	4s	2-Thienyl	Me	356	328	28
20	4t	2-Thienyl	Et	400	386	14
21	4u	2-Pyridinyl	Me	333	336	−3
22	4v	2-Pyridinyl	Et	370	369	1
23	4w	1-Methyl-1 <i>H</i> -benzo[<i>d</i>]imidazol-2-yl	Me	223	227	−4
24	4x	1-Methyl-1 <i>H</i> -benzo[<i>d</i>]imidazol-2-yl	Et	299	285	14

2.2.2. Toxicological Bioassay

The most potent hits in this study, compounds (4a, c, e, f, g, l, m, r, s, t, w and 4x), were tested at 1000 mg kg^{−1} (mouse body weight), with no toxic symptoms or mortality rates being observed after 24 h post-administrations elucidating the safe behavior of the used doses. Thus, the present study recommended that the benzofuran-containing compounds may have the potential to be developed into potent vasodilatory active agents.

3. Experimental Section

3.1. General Information

Melting points were recorded on a Stuart SMP30 melting point apparatus. IR spectra (KBr) were recorded on a JASCO 6100 spectrophotometer, JASCO, Easton, USA. NMR spectra were recorded on a JEOL AS 500 (DMSO-*d*₆, ¹H: 500 MHz, ¹³C: 125 MHz) spectrometer, JEOL USA, Inc. (Pleasanton, CA, USA). Chemical shifts (δ_H) are reported relative to Tetramethylsilane (TMS) as the internal standard. All coupling constant (*J*) values are given in hertz. Chemical shifts (δ_c) are reported relative to CDCl₃ as internal standards. Mass spectra were recorded on a Shimadzu GCMS-QP 1000 EX (EI, 70 eV) spectrometer, Shimadzu corporation, Kyoto, Japan. Elemental microanalyses were performed by using a Vario Elemental analyzer, Elementar Analysensysteme GmbH, Langensfeld, Germany. 2-Acetylbenzofuran [38], 3-(benzofuran-2-yl)-1-phenyl-1*H*-pyrazole-4-carbaldehyde (1) [32] and 2-((3-(benzofuran-2-yl)-1-phenyl-1*H*-pyrazol-4-yl)methylene)malononitrile (1) [32] were prepared according to the previously reported procedures.

3.1.1. Synthesis of 2-((3-(Benzofuran-2-yl)-1-phenyl-1*H*-pyrazol-4-yl)methylene)malononitrile (2)

The formed carbaldehyde 1 (2.88 g, 10 mmol) was stirred in ethanol at room temperature (25–30 °C) for 6 h with malononitrile (0.66 g, 10 mmol) in the presence of few drops of piperidine, the formed precipitate was filtered, dried and recrystallized from *n*-butanol, to afford 2.54 g of compound 2 (75% yield).

3.1.2. Synthesis of 2-Alkoxy-4-(3-(benzofuran-2-yl)-1-phenyl-1*H*-pyrazol-4-yl)-6-phenylpyridine-3-carbonitriles (4a–x)

General Procedure

A mixture of equimolar amounts of 2 (3.36 g, 10 mmol) and methyl aryl ketones 3a–l (10 mmol), in the appropriate alcohol (20 mL) containing sodium (0.46 g, 20 mmol) was stirred at room temperature (25–30 °C) for the proper time controlled by Thin-layer chromatography (TLC). The solid separated was collected, washed with water and crystallized from *n*-butanol to afford the title compounds 4a–x.

4-(3-(Benzofuran-2-yl)-1-phenyl-1H-pyrazol-4-yl)-2-methoxy-6-phenylpyridine-3-carbonitrile (**4a**): yield 1.86 g (39.7%), m.p. 198–200 °C. IR: $\nu_{\max}/\text{cm}^{-1}$ 2213 (C≡N), 1588, 1543 (C=N, C=C). ¹H-NMR (CDCl₃): δ 4.23 (s, 3H), 7.08 (s, 1H), 7.25–7.29 (m, 4H), 7.39–8.04 (m, 6H), 7.09 (d, $J = 7.7$ Hz, 2H), 8.04 (d, $J = 7.7$ Hz, 2H), 8.38 (s, 1H), 8.42 (s, 1H). ¹³C-NMR (CDCl₃): δ 54.7, 93.5, 105.7, 105.8, 111.6, 111.7, 114.6, 119.8, 120.0, 121.4, 123.3, 125.1, 126.7, 127.4, 127.8, 127.9, 128.4, 128.6, 128.7, 129.0, 129.7, 130.6, 139.3, 154.9, 155.1, 157.8, 165.0. MS: m/z (%) 468.31 (M, 0.47). Anal. for C₃₀H₂₀N₄O₂ (468.51); Calcd. C, 76.91; H, 4.30; N, 11.96. Found: C, 76.84; H, 4.26; N, 11.87.

4-(3-(Benzofuran-2-yl)-1-phenyl-1H-pyrazol-4-yl)-2-ethoxy-6-phenylpyridine-3-carbonitrile (**4b**): yield 1.84 g (39%), m.p. 186–188 °C. IR: $\nu_{\max}/\text{cm}^{-1}$: 2215 (C≡N), 1590, 1541 (C=N, C=C). ¹H-NMR (CDCl₃): δ 1.55 (t, $J = 7.6$ Hz, 3H), 4.69 (q, $J = 7.6$ Hz, 2H), 7.05 (s, 1H), 7.20–7.53 (m, 10 H), 7.81–8.10 (m, 4 H), 8.40 (s, 1H), 8.50 (s, 1H). ¹³C-NMR (CDCl₃): δ 14.8, 63.5, 93.6, 105.8, 111.6, 114.3, 116.1, 118.1, 119.0, 120.0, 121.4, 123.3, 125.1, 127.3, 127.8, 128.6, 128.7, 128.9, 129.7, 132.5, 135.4, 138.5, 140.0, 143.0, 147.3, 148.9, 155.1, 157.7, 164.8. MS: m/z (%) 482.25 (M, 20.34). Anal. for C₃₁H₂₂N₄O₂ (482.53); Calcd. C, 77.16; H, 4.60; N, 11.61. Found: C, 77.05; H, 4.57; N, 11.72.

4-(3-(Benzofuran-2-yl)-1-phenyl-1H-pyrazol-4-yl)-6-(4-chlorophenyl)-2-methoxypyridine-3-carbonitrile (**4c**): yield 2.04 g (40.5%), m.p. 259–261 °C. IR: $\nu_{\max}/\text{cm}^{-1}$ 2214 (C≡N), 1588, 1542 (C=N, C=C). ¹H-NMR (DMSO-*d*₆): δ 4.14 (s, 3H), 7.08 (s, 1H), 7.20–7.58 (m, 9H), 7.92 (s, 1H), 8.0 (d, $J = 8$ Hz, 2H), 8.12 (d, $J = 8$ Hz, 2H), 9.1 (s, 1H). MS: m/z (%) 502.11 (M, 0.47). Anal. for C₃₀H₁₉ClN₄O₂ (502.95); Calcd. C, 71.64; H, 3.81; N, 11.14. Found: C, 71.56; H, 3.78; N, 11.18.

4-(3-(Benzofuran-2-yl)-1-phenyl-1H-pyrazol-4-yl)-6-(4-chlorophenyl)-2-ethoxypyridine-3-carbonitrile (**4d**): yield 2.27 g (40.4%), m.p. 199–201 °C. IR: $\nu_{\max}/\text{cm}^{-1}$ 2219 (C≡N), 1588, 1541 (C=N, C=C). ¹H-NMR (CDCl₃): δ 1.54 (t, $J = 6.7$ Hz, 3H), 4.67 (q, $J = 6.7$ Hz, 2H), 7.08 (s, 1H), 7.35–7.53 (m, 10H), 7.81–7.84 (m, 4H), 8.43 (s, 1H). ¹³C-NMR (CDCl₃): δ 14.6, 63.5, 93.8, 105.9, 111.5, 114.1, 116.0, 117.5, 119.9, 121.5, 123.4, 125.2, 127.9, 128.4, 128.6, 129.0, 129.2, 129.8, 135.8, 136.7, 139.2, 148.9, 149.0, 154.9, 156.4, 164.7. MS: m/z (%) 516.30, 518.30 (M, M+2, 1.95, 0.68). Anal. for C₃₁H₂₁ClN₄O₂ (516.98); Calcd. C, 72.02; H, 4.09; N, 10.84. Found: C, 72.14; H, 4.14; N, 10.78.

4-(3-(Benzofuran-2-yl)-1-phenyl-1H-pyrazol-4-yl)-6-(4-bromophenyl)-2-methoxypyridine-3-carbonitrile (**4e**): yield 2.14 g (39%), m.p. 273–275 °C. IR: $\nu_{\max}/\text{cm}^{-1}$ 2217 (C≡N), 1585, 1542 (C=N, C=C). ¹H-NMR (DMSO-*d*₆): δ 4.14 (s, 3H), 7.09 (s, 1H), 7.20–7.73 (m, 10H), 7.96–7.16 (m, 4H), 9.10 (s, 1H). MS: m/z (%) 546.16 (M, 3.22). Anal. for C₃₀H₁₉BrN₄O₂ (547.40); Calcd. C, 65.82; H, 3.50; N, 10.24. Found: C, 65.94; H, 3.38; N, 10.17.

4-(3-(Benzofuran-2-yl)-1-phenyl-1H-pyrazol-4-yl)-6-(4-bromophenyl)-2-ethoxypyridine-3-carbonitrile (**4f**): yield 1.94 g (34.6%), m.p. 207–209 °C. IR: $\nu_{\max}/\text{cm}^{-1}$ 2219 (C≡N), 1588, 1540 (C=N, C=C). ¹H-NMR (CDCl₃): δ 1.54 (t, $J = 6.7$ Hz, 3H), 4.67 (q, $J = 6.7$ Hz, 2H), 7.09 (s, 1H), 7.20–7.52 (m, 10H), 7.77–7.81 (m, 4H), 8.44 (s, 1H). ¹³C-NMR (CDCl₃): δ 14.6, 63.6, 93.9, 105.9, 111.5, 114.1, 115.7, 117.5, 120.0, 121.5, 123.4, 125.2, 127.9, 128.4, 128.8, 129.0, 129.8, 132.2, 136.3, 139.3, 142.4, 147.4, 148.9, 154.9, 156.5, 164.8. MS: m/z (%) 560.40 (M, 0.24). Anal. for C₃₁H₂₁BrN₄O₂ (561.43); Calcd. C, 66.32; H, 3.77; N, 9.98. Found: C, 66.54; H, 3.84; N, 9.82.

4-(3-(benzofuran-2-yl)-1-phenyl-1H-pyrazol-4-yl)-6-(4-fluorophenyl)-2-methoxypyridine-3-carbonitrile (**4g**): yield 1.96 g (40.3%), m.p. 237–239 °C. IR: $\nu_{\max}/\text{cm}^{-1}$ 2215 (C≡N), 1590, 1543 (C=N, C=C). ¹H-NMR (CDCl₃): δ 4.22 (s, 3H), 7.07 (s, 1H), 7.25–7.53 (m, 10H), 7.81–7.93 (m, 4H), 8.44 (s, 1H). MS: m/z (%) 486.31 (M, 1.90). Anal. for C₃₀H₁₉FN₄O₂ (486.5); Calcd. C, 74.06; H, 3.94; N, 11.52. Found: C, 73.95; H, 3.88; N, 11.48.

4-(3-(Benzofuran-2-yl)-1-phenyl-1H-pyrazol-4-yl)-2-ethoxy-6-(4-fluorophenyl)pyridine-3-carbonitrile (**4h**): yield 2.12 g (42.4%), m.p. 204–206 °C. IR: $\nu_{\max}/\text{cm}^{-1}$ 2218 (C≡N), 1592, 1543 (C=N, C=C). ¹H-NMR (CDCl₃): δ 1.53 (t, $J = 7$ Hz, 3H), 4.67 (q, $J = 7$ Hz, 2H), 7.08 (s, 1H), 7.39–7.54 (m, 10 H), 7.81–7.83 (m,

4H), 8.44 (s, 1H). ^{13}C -NMR (CDCl_3): δ 14.6, 63.6, 93.5, 105.9, 111.5, 115.9, 116.1, 120.0, 121.4, 123.4, 125.1, 127.9, 129.0, 129.3, 129.4, 129.8, 139.3, 142.4, 147.4, 148.9, 154.9, 156.6, 163.3, 164.8, 165.3. MS: m/z (%) 500.36 (M, 2.71). Anal. for $\text{C}_{31}\text{H}_{21}\text{FN}_4\text{O}_2$ (500.52); Calcd. C, 74.39; H, 4.23; N, 11.19. Found: C, 74.45; H, 4.18; N, 11.14.

4-(3-(Benzofuran-2-yl)-1-phenyl-1H-pyrazol-4-yl)-2-methoxy-6-p-tolylpyridine-3-carbonitrile (**4i**): yield 2.3 g (47.7%), m.p. 258–260 °C. IR: $\nu_{\text{max}}/\text{cm}^{-1}$ 2218 ($\text{C}\equiv\text{N}$), 1588, 1541 ($\text{C}=\text{N}$, $\text{C}=\text{C}$). ^1H -NMR (CDCl_3): δ 2.39 (s, 3H), 4.22 (s, 3H), 7.06 (s, 1H), 7.22–7.52 (m, 10H), 7.58–7.86 (m, 4H), 8.41 (s, 1H). ^{13}C -NMR (CDCl_3): δ 21.5, 54.7, 93.1, 105.8, 111.6, 114.2, 115.9, 117.6, 120.1, 121.4, 123.3, 125.1, 127.3, 127.9, 128.4, 129.0, 129.7, 134.5, 139.3, 141.0, 147.2, 148.9, 154.5, 157.9, 165.0. MS: m/z (%) 482.27 (M, 30.7). Anal. for $\text{C}_{31}\text{H}_{22}\text{N}_4\text{O}_2$ (482.53): Calcd. C, 77.16; H, 4.60; N, 11.61. Found: C, 77.29; H, 4.42; N, 11.51.

4-(3-(Benzofuran-2-yl)-1-phenyl-1H-pyrazol-4-yl)-2-ethoxy-6-p-tolylpyridine-3-carbonitrile (**4j**): yield 1.92 g (38.7%), m.p. 202–204 °C. IR: $\nu_{\text{max}}/\text{cm}^{-1}$ 2215 ($\text{C}\equiv\text{N}$), 1598, 1543 ($\text{C}=\text{N}$, $\text{C}=\text{C}$). ^1H -NMR (CDCl_3): δ 1.54 (t, $J = 6$ Hz, 3H), 2.39 (s, 3H), 4.69 (q, $J = 6$ Hz, 2H), 7.05 (s, 1H), 7.20–7.56 (m, 10H), 7.81–7.85 (m, 4H), 8.41 (s, 1H). ^{13}C -NMR (CDCl_3): δ 14.7, 21.5, 63.4, 93.2, 105.8, 111.6, 114.0, 116.0, 117.7, 120.0, 121.4, 123.3, 125.1, 127.3, 127.8, 128.4, 129.0, 129.7, 134.6, 139.3, 141.0, 143.0, 147.2, 149.0, 154.9, 157.8, 164.7. MS: m/z (%) 496.22 (M, 5.52). Anal. for $\text{C}_{32}\text{H}_{24}\text{N}_4\text{O}_2$ (496.56): Calcd. C, 77.40; H, 4.87; N, 11.28. Found: C, 77.52; H, 4.76; N, 11.34.

4-(3-(Benzofuran-2-yl)-1-phenyl-1H-pyrazol-4-yl)-2-methoxy-6-(4-methoxyphenyl)pyridine-3-carbonitrile (**4k**): yield 1.86 g (37.3%), m.p. 256–258 °C. IR: $\nu_{\text{max}}/\text{cm}^{-1}$ 2213 ($\text{C}\equiv\text{N}$), 1588, 1543 ($\text{C}=\text{N}$, $\text{C}=\text{C}$). ^1H -NMR ($\text{DMSO}-d_6$): δ 3.80 (s, 3H), 4.13 (s, 3H), 7.04 (s, 1H), 7.20–7.62 (m, 10H), 7.88–8.20 (m, 4H), 9.08 (s, 1H). MS: m/z (%) 498.38 (M, 100). Anal. for $\text{C}_{31}\text{H}_{22}\text{N}_4\text{O}_3$ (498.53); Calcd. C, 74.69; H, 4.45; N, 11.24. Found: C, 74.66; H, 4.38; N, 11.29.

4-(3-(Benzofuran-2-yl)-1-phenyl-1H-pyrazol-4-yl)-2-ethoxy-6-(4-methoxyphenyl)pyridine-3-carbonitrile (**4l**): yield 2.14 g (41.7%), m.p. 168–170 °C. IR: $\nu_{\text{max}}/\text{cm}^{-1}$ 2219 ($\text{C}\equiv\text{N}$), 1589, 1543 ($\text{C}=\text{N}$, $\text{C}=\text{C}$). ^1H -NMR (CDCl_3): δ 1.54 (t, $J = 7$ Hz, 3H), 3.83 (s, 3H), 4.67 (q, $J = 7$ Hz, 2H), 6.90 (s, 1H), 7.05 (s, 1H), 7.45–7.52 (m, 9H), 7.81–7.90 (m, 4H), 8.40 (s, 1H). ^{13}C -NMR (CDCl_3): δ 14.7, 55.5, 63.4, 92.6, 105.8, 111.6, 113.4, 114.3, 117.8, 120, 121.4, 123.3, 125.1, 127.8, 128.4, 128.9, 129, 129.7, 139.3, 142.4, 147.1, 149, 154.9, 157.4, 161.7, 164.7. MS: m/z (%) 512 (M, 22.4). Anal. for $\text{C}_{32}\text{H}_{24}\text{N}_4\text{O}_3$ (512.56); Calcd. C, 74.99; H, 4.72; N, 10.93. Found: C, 74.91; H, 4.71; N, 10.89.

4-(3-(Benzofuran-2-yl)-1-phenyl-1H-pyrazol-4-yl)-6-(1,2,3,4-tetrahydronaphthalen-6-yl)-2-methoxypyridine-3-carbonitrile (**4m**): yield 1.78 g (34%), m.p. 255–257 °C. IR: $\nu_{\text{max}}/\text{cm}^{-1}$ 2221 ($\text{C}\equiv\text{N}$), 1591, 1555 ($\text{C}=\text{N}$, $\text{C}=\text{C}$). ^1H -NMR (CDCl_3): δ 1.58 (s, 2H), 1.79 (s, 2H), 2.69 (s, 2H), 2.78 (s, 2H), 4.22 (s, 3H), 7.06 (s, 1H), 7.24–7.58 (m, 10H), 7.81–7.83 (m, 4H), 8.43 (s, 1H). ^{13}C -NMR (CDCl_3): δ 23.1, 29.6, 54.6, 92.8, 105.9, 111.6, 114.3, 119.9, 121.4, 123.0, 124.5, 125.1, 127.8, 128.1, 128.4, 128.9, 129.7, 129.9, 137.3, 155.0, 158.2, 165.0. Anal. for $\text{C}_{34}\text{H}_{26}\text{N}_4\text{O}_2$ (522.6); Calcd. C, 78.14; H, 5.01; N, 10.72. Found: C, 73.69; H, 4.14; N, 15.56.

4-(3-(Benzofuran-2-yl)-1-phenyl-1H-pyrazol-4-yl)-2-ethoxy-6-(1,2,3,4-tetrahydronaphthalen-6-yl)pyridine-3-carbonitrile (**4n**): Yield 2.16 g (40.3%), m.p. 213–215 °C. IR: $\nu_{\text{max}}/\text{cm}^{-1}$ 2213 ($\text{C}\equiv\text{N}$), 1585, 1542 ($\text{C}=\text{N}$, $\text{C}=\text{C}$). ^1H -NMR (CDCl_3): δ 1.54 (t, $J = 7.7$ Hz, 3H), 1.78 (s, 4H), 2.69 (s, 2H), 2.78 (s, 2H), 4.68 (q, $J = 7.7$ Hz, 2H), 7.05 (s, 1H), 7.12–7.56 (m, 11H), 7.81 (d, $J = 8.5$ Hz, 2H), 8.42 (s, 1H). ^{13}C -NMR (CDCl_3): δ 14.7, 23.1, 23.2, 29.6, 29.6, 63.4, 92.9, 105.9, 111.6, 114.0, 116.0, 118.0, 120.0, 121.4, 123.3, 124.5, 125.1, 127.8, 128.1, 128.9, 129.7, 129.8, 135.0, 137.8, 140.3, 148.5, 149.5, 155.0, 158.2, 164.8. MS: m/z (%) 536.31 (M, 100). Anal. for $\text{C}_{35}\text{H}_{28}\text{N}_4\text{O}_2$ (536.62); Calcd. C, 78.34; H, 5.26; N, 10.44. Found: C, 78.52; H, 5.14; N, 10.57.

4-(3-(Benzofuran-2-yl)-1-phenyl-1H-pyrazol-4-yl)-2-methoxy-6-(1H-pyrrol-2-yl)pyridine-3-carbonitrile (**4o**): yield 1.86 g (40.6%), m.p. 187–189 °C. IR: $\nu_{\text{max}}/\text{cm}^{-1}$ 2218 ($\text{C}\equiv\text{N}$), 1587, 1539 ($\text{C}=\text{N}$, $\text{C}=\text{C}$). ^1H -NMR

(CDCl₃): δ 3.97 (s, 3H), 7.06 (s, 1H), 7.29–7.55 (m, 10H), 7.59–7.82 (m, 2H), 8.45 (s, 1H), 9.05 (s, 1H). ¹³C-NMR (CDCl₃): δ 54.5, 102.0, 106.3, 111.6, 115.4, 117.0, 120.0, 121.7, 123.6, 125.4, 128.2, 128.4, 129.8, 129.9, 138.9, 139.1, 145.7, 148.9, 155.3, 162.4. MS: m/z (%) 457.25 (M, 1.93). Anal. for C₂₈H₁₉N₅O₂ (457.48); Calcd. C, 73.51; H, 4.19; N, 15.31. Found: C, 73.69; H, 4.14; N, 15.56.

4-(3-(Benzofuran-2-yl)-1-phenyl-1H-pyrazol-4-yl)-2-ethoxy-6-(1H-pyrrol-2-yl)pyridine-3-carbonitrile (**4p**): yield 1.84 g (39%), m.p. 208–210 °C. IR: $\nu_{\max}/\text{cm}^{-1}$ 2217 (C≡N), 1588, 1538 (C=N, C=C). ¹H-NMR (CDCl₃): δ 1.53 (t, $J = 7.7$ Hz, 3H), 4.64 (q, $J = 7.7$ Hz, 2H), 7.05 (s, 1H), 7.20–7.30 (m, 4H), 7.46–7.54 (m, 8H), 7.81 (d, 2H), 8.40 (s, 1H). ¹³C-NMR (CDCl₃): δ 14.6, 63.8, 93.0, 105.8, 111.6, 112.7, 120.1, 121.4, 123.3, 125.1, 127.1, 127.9, 128.6, 129.0, 129.7, 130.0, 139.3, 142.4, 143.4, 147.2, 148.8, 152.9, 154.9, 164.7. MS: m/z (%) 471.37 (M, 100). Anal. for C₂₉H₂₁N₅O₂ (471.51); Calcd. C, 73.87; H, 4.49; N, 14.85. Found: C, 73.75; H, 4.43; N, 14.88.

4-(3-(Benzofuran-2-yl)-1-phenyl-1H-pyrazol-4-yl)-6-(furan-2-yl)-2-methoxy-pyridine-3-carbonitrile (**4q**): yield 1.88 g (41%), m.p. 246–248 °C. IR: $\nu_{\max}/\text{cm}^{-1}$ 2217 (C≡N), 1588, 1538 (C=N, C=C). ¹H-NMR (CDCl₃): δ 4.21 (s, 3H), 6.54 (s, 1H), 7.05 (s, 1H), 7.20–7.53 (m, 10H), 7.80 (d, 2H), 8.35 (s, 1H). ¹³C-NMR (CDCl₃): δ 54.7, 93.3, 105.7, 111.6, 112.3, 112.6, 117.4, 120.0, 121.4, 123.2, 125.0, 127.9, 128.4, 129.0, 129.7, 139.3, 142.4, 145.1, 147.6, 148.7, 149.3, 152.5, 154.9, 165.1. MS: m/z (%) 458.21 (M, 100). Anal. for C₂₈H₁₈N₄O₃ (458.47); Calcd. C, 73.35; H, 3.96; N, 12.22. Found: C, 71.22; H, 4.14; N, 11.49.

4-(3-(Benzofuran-2-yl)-1-phenyl-1H-pyrazol-4-yl)-2-ethoxy-6-(furan-2-yl)pyridine-3-carbonitrile (**4r**): Yield 2.14 g (45.3%), m.p. 174–176 °C. IR: $\nu_{\max}/\text{cm}^{-1}$ 2216 (C≡N), 1590, 1521 (C=N, C=C). ¹H-NMR (CDCl₃): δ 1.51 (t, $J = 7$ Hz, 3H), 4.62 (q, $J = 7$ Hz, 2H), 6.53 (s, 1H), 7.00 (s, 1H), 7.15–7.30 (m, 3H), 7.39–7.55 (m, 7H), 7.81 (d, 2H), 8.35 (s, 1H). Anal. for C₂₉H₂₀N₄O₃ (472.49); Calcd. C, 73.72; H, 4.27; N, 11.86. Found: C, 73.65; H, 4.29; N, 11.83.

4-(3-(Benzofuran-2-yl)-1-phenyl-1H-pyrazol-4-yl)-2-methoxy-6-(thiophen-2-yl)pyridine-3-carbonitrile (**4s**): yield 1.58 g (33.3%), m.p. 232–234 °C. IR: $\nu_{\max}/\text{cm}^{-1}$ 2211 (C≡N), 1629, 1523 (C=N, C=C). ¹H-NMR (CDCl₃): δ 4.19 (s, 3H), 7.06 (s, 1H), 7.25–7.52 (m, 11H), 7.81 (d, 2H), 8.40 (s, 1H). ¹³C-NMR (CDCl₃): δ 54.8, 92.9, 105.8, 111.6, 112.9, 120.1, 121.4, 123.3, 127.2, 127.9, 128.6, 129.1, 129.7, 130.1, 139.3, 142.4, 143.2, 148.8, 153.0, 154.9, 165.0. MS: m/z (%) 474.18 (M, 100). Anal. for C₂₈H₁₈N₄O₂S (474.53); Calcd. C, 70.87; H, 3.82; N, 11.81. Found: C, 70.79; H, 3.74; N, 11.74.

4-(3-(Benzofuran-2-yl)-1-phenyl-1H-pyrazol-4-yl)-2-ethoxy-6-(thiophen-2-yl)pyridine-3-carbonitrile (**4t**): Yield 2.06 g (42.2%), m.p. 202–204 °C. IR: $\nu_{\max}/\text{cm}^{-1}$ 2217 (C≡N), 1591, 1546 (C=N, C=C). ¹H-NMR (CDCl₃): ¹H-NMR (CDCl₃): δ 1.52 (t, $J = 7$ Hz, 3H), 4.63 (q, $J = 7$ Hz, 2H), 6.35 (s, 1H), 6.65 (s, 1H), 7.26–7.52 (m, 3H), 7.64–7.83 (m, 7H), 8.25 (d, $J = 8$ Hz, 2H), 8.36 (s, 1H), 9.65 (s, 1H). ¹³C-NMR (CDCl₃): δ 14.6, 63.8, 93.0, 105.8, 111.6, 112.7, 115.5, 117.5, 120.1, 121.4, 123.4, 125.1, 127.1, 127.9, 128.6, 129.0, 129.7, 130.0, 139.3, 142.4, 143.4, 147.2, 148.8, 153.0, 155.0, 165.0. MS: m/z (%) 488.34 (M, 100). Anal. for C₂₉H₂₀N₄O₂S (488.56); Calcd. C, 71.29; H, 4.13; N, 11.47. Found: C, 71.22; H, 4.14; N, 11.49.

4-(3-(Benzofuran-2-yl)-1-phenyl-1H-pyrazol-4-yl)-2-methoxy-6-(pyridin-2-yl)pyridine-3-carbonitrile (**4u**): Yield 1.85 g (39.4%), m.p. 275–277 °C. IR: $\nu_{\max}/\text{cm}^{-1}$ 2218 (C≡N), 1588, 1545 (C=N, C=C). ¹H-NMR (DMSO-*d*₆): δ 4.18 (s, 3H), 7.09 (s, 1H), 7.25–7.62 (m, 10H), 7.98 (d, $J = 6.7$ Hz, 2H), 8.26 (s, 1H), 8.66 (s, 1H), 9.15 (s, 1H). MS: m/z (%) 469.39 (M, 100). Anal. for C₂₉H₁₉N₅O₂ (469.49); Calcd. C, 74.19; H, 4.08; N, 14.92. Found: C, 74.24; H, 4.15; N, 14.86.

4-(3-(Benzofuran-2-yl)-1-phenyl-1H-pyrazol-4-yl)-2-ethoxy-6-(pyridin-2-yl)pyridine-3-carbonitrile (**4v**): yield 1.75 g (36.2%), m.p. 204–206 °C. IR: $\nu_{\max}/\text{cm}^{-1}$ 2219 (C≡N), 1589, 1543 (C=N, C=C). ¹H-NMR (CDCl₃): δ 1.55 (t, $J = 6.7$ Hz, 3H), 4.69 (q, $J = 6.7$ Hz, 2H), 7.03 (s, 1H), 7.19–7.53 (m, 13H), 7.82 (d, $J = 8.6$ Hz, 2H), 8.27–8.35 (m, 2H), 8.65 (s, 1H). ¹³C-NMR (CDCl₃): δ 14.6, 63.7, 95.8, 104.9, 105.5, 111.6, 119.8, 120.0, 121.3, 123.1, 124.8, 128.9, 129.7, 137.0, 139.4, 142.5, 142.6, 148.1, 149.6, 154.3, 156.5, 164.6. MS: m/z (%)

483.25 (M, 100). Anal. for C₃₀H₂₁N₅O₂ (483.52); Calcd. C, 74.52; H, 4.38; N, 14.48. Found: C, 74.36; H, 4.24; N, 11.56.

4-(3-(Benzofuran-2-yl)-1-phenyl-1H-pyrazol-4-yl)-2-methoxy-6-(1-methyl-1H-benzo[d]imidazole-2-yl)pyridine-3-carbonitrile (**4w**): yield 2.05 g (39.2%), m.p. 295–297 °C. IR: $\nu_{\max}/\text{cm}^{-1}$ 2214 (C≡N), 1586, 1538 (C=N, C=C). ¹H-NMR (CDCl₃): δ 4.18 (s, 3H), 4.35 (s, 3H), 7.14 (s, 1H), 7.27–8.01 (m, 13H), 8.26 (s, 1H), 9.16 (s, 1H). MS: m/z (%) 522.1 (M, 20.5). Anal. for C₃₂H₂₂N₆O₂ (522.56); Calcd. C, 73.55; H, 4.24; N, 16.08. Found: C, 73.49; H, 4.22; N, 16.13.

4-(3-(Benzofuran-2-yl)-1-phenyl-1H-pyrazol-4-yl)-2-ethoxy-6-(1-methyl-1H-benzo[d]imidazol-2-yl)pyridine-3-carbonitrile (**4x**): yield 2.12 g (39.5%), m.p. 247–249 °C. IR: $\nu_{\max}/\text{cm}^{-1}$ 2218 (C≡N), 1587, 1539 (C=N, C=C). ¹H-NMR (CDCl₃): δ 1.56 (t, $J = 7$ Hz, 3H), 4.36 (q, $J = 7$ Hz, 2H), 4.64 (s, 3H), 7.1 (s, 1H), 7.20–7.53 (m, 11H, Ar-H), 7.77, 7.83 (dd, 2H, $J = 7.65$, $J = 7.65$, Ar-H), 8.33 (s, 1H), 8.39 (s, 1H). ¹³C-NMR (CDCl₃): δ 14.6, 33.2, 64.1, 95.9, 105.4, 110.1, 111.7, 118.7, 120.0, 120.6, 121.4, 123.1, 123.3, 124.4, 124.8, 127.8, 128.9, 129.7, 137.5, 139.3, 142.5, 142.7, 148.1, 148.3, 148.9, 150.7, 155.0, 164.3. MS: m/z (%) 536.44 (M, 100). Anal. for C₃₃H₂₄N₆O₂ (536.58); Calcd. C, 73.87; H, 4.51; N, 15.66. Found: C, 73.91; H, 4.45; N, 15.58.

3.2. Vasodilation Activity Screening

The vasodilation activity screening procedures were carried out according to the standard reported techniques [35] by testing the effects of the synthesized 2-alkoxy-4-aryl-6-(benzofuran-2-yl)-3-pyridinecarbonitriles **4a–x** on isolated thoracic aortic rings of male Wistar rats (250–350 g). After light ether anesthesia, the rats were sacrificed by cervical dislocation. The aortae were immediately excised, freed of extraneous tissues and prepared for isometric tension recording. Aorta was cut into (3–5 mm width) rings and each ring was placed in a vertical chamber “10 mL jacketed automatic multi-chamber organ bath system (Model no. ML870B6/C, Panlab, Spain)” filled with Krebs solution composed of (in mM): NaCl, 118.0; KCl, 4.7; NaHCO₃, 25.0; CaCl₂, 1.8; NaH₂PO₄, 1.2; MgSO₄, 1.2; glucose, 11.0 and oxygenated with carbogen gas (95% O₂/5% CO₂) at 37 ± 0.5 °C. Each aortic ring was mounted between two stainless steel hooks passed through its lumen. The lower hook was fixed between two plates, while the upper one was attached to a force displacement transducer (Model no. MLT0201, Panlab, Spain) connected to an amplifier (PowerLab, AD Instruments Pty., Ltd. Victoria, Australia), which is connected to a computer. The chart for Windows (v 3.4) software was used to record and elaborate data. Preparations were stabilized under 2 g resting tension during 2 h and then the contracture response to norepinephrine hydrochloride (10^{−6} M) was measured before and after exposure to increasing concentrations of the tested synthesized compounds. The tested compounds were dissolved in dimethylsulfoxide (DMSO) as stock solution (10 mL of 0.005 M). Control experiments were performed in the presence of DMSO alone, at the same concentrations as those used with the derivatives tested, which demonstrated that the solvent did not affect the contractile response of isolated aorta. The observed vasodilation activity screening data are reported and the potency (IC₅₀, concentration necessary for 50% reduction of maximal norepinephrine hydrochloride induced contracture) was calculated in three successful replicates and the observed vasodilation activity data expressed as IC₅₀ has determined mathematically from the dose response curve of each tested compound (Table 1), (Figures S1 and S2 of Supplementary Materials) and the potency (IC₅₀, concentration necessary for 50% reduction of maximal norepinephrine hydrochloride-induced contracture) was determined. This experiment was carried out in according to recommendations in the Guide for the Care and Use of Laboratory Animals of the National Institutes of Health (NIH publication No. 85–23, revised 1996) and under regulations of the Animal Care and Use of National Research Centre in Egypt.

2D-QSAR Study

The QSAR study was undertaken using comprehensive descriptors for structural and statistical analysis (CODESSA PRO) software employing the synthesized compounds **4a–x** of the present

study (Table 3). Geometry of the compounds was optimized using molecular mechanics force field (MM⁺) followed by the semiempirical AM1 method implemented in the HyperChem 8.0 package. The structures were fully optimized without fixing any parameters, thus bringing all geometric variables to their equilibrium values. The energy minimization protocol employed the Polake–Ribiere conjugated gradient algorithm. Convergence to a local minimum was achieved when the energy gradient was ≤ 0.01 kcal/mol. The Restricted Hartree–Fock (RHF) method was used in spin-pairing for the two semiempirical tools [39–44]. The resulting output files were exported to CODESSA PRO that includes MOPAC capability for final geometry optimization. CODESSA PRO calculated 797 molecular descriptors including constitutional, topological, geometrical, charge-related, semiempirical, thermodynamic, molecular-type, atomic-type and bond-type descriptors for the exported 24 bioactive benzofuran-based hybrids **4a–x**, which were used in the present study. Different mathematical transformations of the experimentally observed property/activity (IC₅₀, μ M, which is the concentration necessary for 50% reduction of maximal norepinephrine hydrochloride induced contracture) of the training set compounds were utilized for the present QSAR modeling determination including property (IC₅₀, μ M), 1/property, log(property) and 1/log(property) values in searching for the best QSAR models. Best multilinear regression (BMLR) was utilized, which is a stepwise search for the best *n*-parameter regression equations (where, *n* stands for the number of descriptors used), based on the highest *R*² (squared correlation coefficient), *R*²_{cvOO} (squared cross-validation “leave one-out, LOO” coefficient), *R*²_{cvMO} (squared cross-validation “leave many-out, LMO” coefficient), *F* (Fisher statistical significance criteria) values, and *s*² (standard deviation). The QSAR models, with up to four descriptor models describing the bioactivity of the vasodilatory active agents were generated (obeying the thumb rule of 6:1, which is the ratio between the data points and the number of QSAR descriptor models). Statistical characteristics of the QSAR models are presented in Table 2. The established QSAR model is statistically significant. The descriptors are sorted in descending order of the respective values of the Student’s *t*-criterion, which is a widely accepted measure of statistical significance of individual parameters in multiple linear regressions. Figure 2 exhibits the QSAR multilinear model plot of correlation representing the observed vs. predicted 1/IC₅₀ values for vasodilatory active agents. The scattered plots are uniformly distributed, covering ranges, Observed 0.00221–0.00448; Predicted 0.00255–0.004411/IC₅₀ units.

3.3. Toxicological Bioassay

Toxicological bioassay of the most promising vasodilatory active compounds (**4a**, **c**, **e**, **f**, **g**, **l**, **m**, **r**, **s**, **t**, **w** and **4x**) was determined using the standard reported method in mice [45]. Albino mice weighing 25–30 g were divided in 13 groups of 6 mice each. Administrations of the tested compounds dissolved in saline solution (0.9%) by the aid of few drops of Tween 80 were given intraperitoneally in 1000 mg kg^{−1} (mouse body weight). The control group was given saline solution only with few drops of Tween 80. The toxic symptoms and mortality rates were recorded 24 h post-administration in each group.

4. Conclusions

The required 2-alkyloxy-pyridine-3-carbonitrile hybrids (**4a–x**) were designed and synthesized via the condensation reaction of aromatic ketones **3a–l** with 2-((3-(benzofuran-2-yl)-1-phenyl-1*H*-pyrazol-4-yl)methylene)malononitrile (**2**) in the presence of sufficient amount of sodium alkoxide in the corresponding alcohol. The compounds have evaluated for their vasodilation activity adopting the standard technique “using isolated thoracic aortic rings of rats precontracted with norepinephrine hydrochloride”. Some compounds revealed a noteworthy activity, with compounds **4w**, **4e**, **4r**, **4s**, **4f** and **4g** believed to be the most active hits in this study. “IC₅₀, concentration necessary for 50% reduction of maximal norepinephrine hydrochloride induced contracture = 223, 253, 254, 268, 267 and 275 μ M, respectively”, compared with amidarone hydrochloride, the reference standard used (IC₅₀ = 300 μ M). The CODESSA PRO program was utilized to achieve a statistically significant

2D-QSAR model describing the bioactivity of the newly synthesized analogues **4a–x**, and afforded an excellent predictive and statistically vital four-crucial 4 descriptor model ($R^2 = 0.816$, $R^2_{\text{observed}} = 0.731$, $R^2_{\text{predicted}} = 0.772$). It is obvious that the 2D-QSAR study supported the attained model, so the applicability of benzofuran-based hybrids incorporating the 3-pyridinecarbonitrile function have potential to be developed into vasorelaxant active agents.

Supplementary Materials: Supplementary materials are available online.

Acknowledgments: The project was financially supported by King Saud University, Vice Deanship of Research Chairs. The project was also financially supported by National Research Centre, Dokki, Cairo 12622, Egypt, under project No. 110-10-312.

Author Contributions: The listed authors contributed to this work as described in the following. A.M.S. and S.S.A.E.-k. carried out the synthetic work, interpreted the results and prepared the manuscript; N.M.K. and M.A.A.-O. interpreted the results and cooperated in the preparation of the manuscript, and D.O.S. carried and interpreted the results of the biological activities. All authors read and approved the final manuscript.

Conflicts of Interest: The authors declare no conflicts of interest

References

1. Garovic, V.D.; Hayman, S.R. Hypertension in pregnancy: An emerging risk factor for cardiovascular disease. *Nat. Clin. Pract. Nephrol.* **2007**, *3*, 613–622. [CrossRef] [PubMed]
2. Kummerle, A.E.; Raimundo, J.M.; Leal, C.M.; Da Silva, G.S.; Balliano, T.L.; Pereira, M.A.; De Simone, C.A.; Sudo, R.T.; Zapata-Sudo, G.; Fraga, C.A.; et al. Studies towards the identification of putative bioactive conformation of potent vasodilator arylidene *N*-acylhydrazone derivatives. *Eur. J. Med. Chem.* **2009**, *44*, 4004–4009. [CrossRef] [PubMed]
3. World Health Organization. Media Centre. Available online: http://www.who.int/mediacentre/news/releases/2012/world_health_statistics_20120516/en/4004-4009 (accessed on 14 February 2016).
4. Da Silva, V.J.; Viana, P.C.; Alves, R.M.; Salgado, H.C.; Montano, N.; Fazan, R.J. Antihypertensive action of amiodarone in spontaneously hypertensive rats. *Hypertension* **2001**, *38*, 597–601. [CrossRef]
5. Almeida, M.R.; Lima, E.O.; da Silva, V.J.; Campos, M.G.; Antunes, L.M.; Salman, A.K.; Dias, F.L. Genotoxic studies in hypertensive and normotensive rats treated with amiodarone. *Mutat. Res.* **2008**, *657*, 155–159. [CrossRef] [PubMed]
6. World Health Organization. Cardiovascular Disease. Available online: http://www.who.int/topics/cardiovascular_diseases/en/ (accessed on 22 March 2016).
7. Kashyap, M.K.; Yadav, V.; Sherawat, B.S.; Jain, S.; Kumari, S.; Khullar, M.; Sharma, P.C.; Nath, R. Different antioxidants status, total antioxidant power and free radicals in essential hypertension. *Mol. Cell. Biochem.* **2005**, *277*, 89–99. [CrossRef] [PubMed]
8. Wang, R.; Shamloul, R.; Wang, X.; Meng, Q.; Wu, L. Sustained normalization of high blood pressure in spontaneously hypertensive rats by implanted hemin pump. *Hypertension* **2006**, *48*, 685–692. [CrossRef] [PubMed]
9. Carlsson, B.; Singh, B.N.; Temciuc, M.; Nilsson, S.; Li, Y.-L.; Mellin, C.; Malm, J. Synthesis and preliminary characterization of a novel antiarrhythmic compound (KB130015) with an improved toxicity profile compared with amiodarone. *J. Med. Chem.* **2002**, *45*, 623–630. [CrossRef] [PubMed]
10. Mubagwa, K.; Macianskiene, R.; Viappiani, S.; Gendviliene, V.; Carlsson, B.; Brandts, B. KB130015, a new amiodarone derivative with multiple effects on cardiac ion channels. *Cardiovasc. Drug Rev.* **2003**, *21*, 216–235. [CrossRef] [PubMed]
11. Guiraudou, P.; CosnierPucheu, S.C.; Gayraud, R.; Gautier, P.; Roccon, A.; Herbert, J.M.; Nisato, D. Involvement of nitric oxide in amiodarone- and dronedarone-induced coronary vasodilation in guinea pig heart. *Eur. J. Pharmacol.* **2004**, *496*, 119–127. [CrossRef] [PubMed]
12. Kodama, I.; Kamiya, K.; Toyama, J. Amiodarone: Ionic and cellular mechanisms of action of the most promising class III agent. *Am. J. Cardiol.* **1999**, *84*, 20–28. [CrossRef]
13. Grossmann, M.; Dobrev, D.; Kirch, W. Amiodarone causes endothelium-dependent vasodilation in human hand veins in vivo. *Clin. Pharmacol. Ther.* **1998**, *64*, 302–311. [CrossRef]

14. Massie, B.M.; Fisher, S.G.; Deedwania, P.C.; Singh, B.N.; Fletcher, R.D.; Singh, S.N. Effect of amiodarone on clinical status and left ventricular function in patients with congestive heart failure. *Circulation* **1996**, *93*, 2128–2134. [[CrossRef](#)] [[PubMed](#)]
15. Gessner, G.; Heller, R.; Hoshi, T.; Heinemann, S.H. The amiodarone derivative 2-methyl-3-(3,5-diiodo-4-carboxymethoxybenzyl)benzofuran (KB130015) opens large-conductance Ca^{2+} -activated K^{+} channels and relaxes vascular smooth muscle. *Eur. J. Pharm.* **2007**, *555*, 185–193. [[CrossRef](#)] [[PubMed](#)]
16. Hanafy, D.A.; Chen, Y.; Chang, S.; Lu, Y.; Lin, Y.; Kao, Y.; Chen, S.; Chen, Y. Different effects of dronedarone and amiodarone on pulmonary vein electrophysiology, mechanical properties and H_2O_2 -induced arrhythmogenicity. *Eur. J. Pharm.* **2013**, *702*, 103–108. [[CrossRef](#)] [[PubMed](#)]
17. Stewart, S.; Hart, C.L.; Hole, D.J.; McMurray, J.J. A population-based study of the long-term risks associated with atrial fibrillation: 20-year follow-up of the Renfrew/Paisley study. *Am. J. Med.* **2002**, *113*, 359–364. [[CrossRef](#)]
18. Hayta, S.A.; Arisoy, M.; Arpacı, O.T.; Yildiz, I.; Aki, E.; Ozkan, S.; Kaynak, F. Synthesis, antimicrobial activity, pharmacophore analysis of some new 2-(substitutedphenyl/benzyl)-5-[(2-benzofuryl)carboxamido]benzoxazoles. *Eur. J. Med. Chem.* **2008**, *43*, 2568–2578. [[CrossRef](#)] [[PubMed](#)]
19. Manna, K.; Agrawal, Y.K. Microwave assisted synthesis of new indophenazine 1,3,5-trisubstituted pyrazoline derivatives of benzofuran and their antimicrobial activity. *Bioorg. Med. Chem. Lett.* **2009**, *19*, 2688–2692. [[CrossRef](#)] [[PubMed](#)]
20. Xie, Y.; Kumar, D.; Bodduri, V.D.; Tarani, P.S.; Zhao, B.; Miao, J.; Jang, K.; Shin, D. Microwave-assisted parallel synthesis of benzofuran-2-carboxamide derivatives bearing anti-inflammatory, analgesic and antipyretic agents. *Tetrahed. Lett.* **2014**, *55*, 2796–2800. [[CrossRef](#)]
21. El-Sawy, E.R.; Ebaid, M.S.; Abo-Salem, H.M.; Al-Sehemi, A.G.; Mandour, A.H. Synthesis, anti-inflammatory, analgesic and anticonvulsant activities of some new 4,6-dimethoxy-5-(heterocycles)benzofuran starting from naturally occurring. *Arab. J. Chem.* **2014**, *7*, 914–923. [[CrossRef](#)]
22. Thevenin, M.; Thoret, S.; Grellier, P.; Dubois, J. Synthesis of polysubstitutedbenzofuran derivatives as novel inhibitors of parasitic growth. *Bioorg. Med. Chem.* **2013**, *21*, 4885–4892. [[CrossRef](#)] [[PubMed](#)]
23. Feher, D.; Barlow, R.S.; McAtee, J.; Hemscheidt, T.K. Highly brominated antimicrobial metabolites from a marine *Pseudoalteromonas* sp. *J. Nat. Prod.* **2010**, *73*, 1963–1966. [[CrossRef](#)] [[PubMed](#)]
24. Galal, S.A.; Abd El-All, A.S.; Abdallah, M.M.; El-Diwani, H.I. Synthesis of potent antitumor and antiviral benzofuran derivatives. *Bioorg. Med. Chem. Lett.* **2009**, *19*, 2420–2628. [[CrossRef](#)] [[PubMed](#)]
25. Xie, F.; Zhu, H.; Zhang, H.; Lang, Q.; Tang, L.; Huang, Q.; Yu, L. In vitro and in vivo characterization of a benzofuran derivative, a potential anticancer agent, as a novel Aurora B kinase inhibitor. *Eur. J. Med. Chem.* **2015**, *89*, 310–319. [[CrossRef](#)] [[PubMed](#)]
26. Kleemann, A.; Engel, J.; Kutscher, B.; Reichert, D. *Pharmaceutical Substances: Syntheses Patents Applications*, 3rd ed.; Thieme, Stuttgart: New York, NY, USA, 1999.
27. Girgis, A.S.; Kalmouch, A.; Ellithy, M. Synthesis of novel vasodilatory active nicotinate esters with amino acid function. *Bioorg. Med. Chem.* **2006**, *14*, 8488–8494. [[CrossRef](#)] [[PubMed](#)]
28. Nofal, Z.M.; Srour, A.M.; El-Eraky, W.I.; Saleh, D.O.; Girgis, A.S. Rational design, synthesis and QSAR study of vasorelaxant active 3-pyridinecarbonitriles incorporating 1H-benzimidazol-2-yl function. *Eur. J. Med. Chem.* **2013**, *63*, 14–21. [[CrossRef](#)] [[PubMed](#)]
29. Hassan, G.S.; Abdel Rahman, D.E.; Saleh, D.O.; Abdel Jaleel, G.A. Benzofuran–Morpholinomethyl–Pyrazoline Hybrids as a New Class of Vasorelaxant Agents: Synthesis and Quantitative Structure–Activity Relationship Study. *Chem. Pharm. Bull.* **2013**, *62*, 1238–1251. [[CrossRef](#)]
30. Matsui, A.; Matsuo, H.; Takanaga, H.; Sasaki, S.; Maeda, M.; Sawada, Y. Prediction of catalepsies induced by amiodarone, aprindine and procaine: Similarity in conformation of diethylaminoethyl side chain. *J. Pharmacol. Exp. Ther.* **1998**, *287*, 725–732. [[PubMed](#)]
31. Srour, A.M.; Abd El-Karim, S.S.; Saleh, D.O.; El-Eraky, W.I.; Nofal, Z.M. Rational design, synthesis and 2D-QSAR study of novel vasorelaxant active benzofuran-pyridine hybrids. *Bioorg. Med. Chem. Lett.* **2016**, *26*, 2557. [[CrossRef](#)] [[PubMed](#)]
32. El-Zahar, M.I.; Abd El-Karim, S.S.; Anwar, M.M. Synthesis and cytotoxicity screening of some novel benzofuranoyl-pyrazole derivatives against liver and cervix carcinoma cell lines. *S. Afr. J. Chem.* **2009**, *62*, 189–199.

33. Oliferenko, P.V.; Oliferenko, A.A.; Girgis, A.S.; Saleh, D.O.; Srour, A.M.; George, R.F.; Pillai, G.G.; Panda, C.S.; Hall, C.D.; Katritzky, A.R. Synthesis, bioassay, and molecular field topology analysis of diverse vasodilatory heterocycles. *J. Chem. Inf. Model.* **2014**, *54*, 1103–1116. [[CrossRef](#)] [[PubMed](#)]
34. University of Florida 2001–2005, CODESSA PRO. Available online: <http://www.codessa-pro.com/index.htm> (accessed on 20 July 2017).
35. Panda, S.S.; Liaqat, S.; Girgis, A.S.; Samir, A.; Hall, C.D.; Katritzky, A.R. Novel antibacterial active quinolone–fluoroquinolone conjugates and 2D-QSAR studies. *Bioorg. Med. Chem. Lett.* **2015**, *25*, 3816–3821. [[CrossRef](#)] [[PubMed](#)]
36. Girgis, A.S.; Pand, S.S.; Ahmed Farag, I.S.; El-Shabiny, A.M.; Moustafa, A.M.; Pillai, G.G.; Panda, C.S.; Hall, C.D.; Katritzky, A.R. Synthesis, and QSAR analysis of anti-oncological active spiro-alkaloids. *Org. Biomol. Chem.* **2015**, *13*, 1741–1753. [[CrossRef](#)] [[PubMed](#)]
37. Girgis, A.S.; Mishriky, N.; Farag, A.M.; El-Eraky, W.I.; Farag, H. Synthesis of new 3-pyridinecarboxylates of potential vasodilation properties. *Eur. J. Med. Chem.* **2008**, *43*, 1818–1827. [[CrossRef](#)] [[PubMed](#)]
38. Raj, P.A.; Suddendra, G.; Shakeel, A.S.; Girish, M. Synthesis of new benzofuran derivatives and their in vitro evaluation for antimicrobial activity. *IJDFR* **2012**, *3*, 135–147.
39. Girgis, A.S.; Panda, S.S.; Srour, A.M.; Farag, H.; Ismail, N.M.; Elgendy, A.M.; Abdel-Aziz, M.; Katritzky, A.R. Rational design, synthesis and molecular modeling studies of novel anti-oncological alkaloids against melanoma. *Org. Biomol. Chem.* **2015**, *13*, 6619–6633. [[CrossRef](#)] [[PubMed](#)]
40. Girgis, A.S.; Panda, S.S.; Aziz, M.N.; Steel, P.J.; Hall, C.D.; Katritzky, A.R. Rational design, synthesis, and 2D-QSAR study of anti-oncological alkaloids against hepatoma and cervical carcinoma. *RSC Adv.* **2015**, *5*, 28554–28569. [[CrossRef](#)]
41. Girgis, A.S.; Panda, S.S.; Shalaby, E.M.; Mabied, A.F.; Steel, P.J.; Hall, C.D.; Katritzky, A.R. Regioselective synthesis and theoretical studies of an anti-neoplastic fluoro-substituted dispiro-oxindole. *RSC Adv.* **2015**, *5*, 14780–14787. [[CrossRef](#)]
42. Girgis, A.S.; Aziz, M.N.; Shalaby, E.M.; Saleh, D.O.; Mishriky, N.; El-Eraky, W.I.; Farag, I.S. Molecular structure studies of novel bronchodilatory active 4-azafluorenes. *Z. Kristallog.* **2016**, *231*, 179–187. [[CrossRef](#)]
43. Girgis, A.S.; Mabied, A.F.; Stawinski, J.; Hegazy, L.; George, R.F.; Farag, H.; Shalaby, E.M.; Farag, I.S. Synthesis and DFT studies of an antitumor active spiro-oxindole. *N. J. Chem.* **2015**, *39*, 8017–8027. [[CrossRef](#)]
44. Shalaby, E.M.; Girgis, A.S.; Moustafa, A.M.; ElShaabiny, A.M.; El-Gendy, B.E.; Mabied, A.F.; Farag, I.S. Regioselective synthesis, stereochemical structure, spectroscopic characterization and geometry optimization of dispiro[3H-indole-3,2'-pyrrolidine-3',3''-piperidines]. *J. Mol. Struct.* **2014**, *1075*, 327–334. [[CrossRef](#)]
45. Tiwari, A.D.; Panda, S.S.; Girgis, A.S.; Sahu, S.; George, R.F.; Srour, A.M.; La Starza, B.; Asiri, A.M.; Hall, C.D.; Katritzky, A.R. Microwave assisted synthesis and QSAR study of novel NSAID acetaminophen conjugates with amino acid linkers. *Org. Biomol. Chem.* **2014**, *12*, 7238–7249. [[CrossRef](#)] [[PubMed](#)]

Sample Availability: Samples of which all the compounds are available from the authors.



© 2017 by the authors. Licensee MDPI, Basel, Switzerland. This article is an open access article distributed under the terms and conditions of the Creative Commons Attribution (CC BY) license (<http://creativecommons.org/licenses/by/4.0/>).